Journal of Statistical Physics, Vol. 81, Nos. 1/2, 1995

An Improved Incompressible Lattice Boltzmann Model for Time-Independent Flows

Qisu Zou,[1,2] Shuling Hou,[1,3] Shiyi Chen,[1,4] and Gary D. Doolen[1]

Received November 2, 1994; final April 11, 1995

It is well known that the lattice Boltzmann equation method (LBE) can model the incompressible Navier–Stokes (NS) equations in the limit where density goes to a constant. In a LBE simulation, however, the density cannot be constant because pressure is equal to density times the square of sound speed, hence a compressibility error seems inevitable for the LBE to model incompressible flows. This work uses a modified equilibrium distribution and a modified velocity to construct an LBE which models time-independent (steady) incompressible flows with significantly reduced compressibility error. Computational results in 2D cavity flow and in a 2D flow with an exact solution are reported.

KEY WORDS: Lattice Boltzmann method; incompressible flows; steady flows.

1. INTRODUCTION

The lattice gas automata (LGA) and the lattice Boltzmann equation (LBE) methods have become alternative computational methods for studying transport phenomena. Since their appearance, numerical simulations have been performed yielding qualitatively correct results. Recently, more careful simulation and quantitative comparison with traditional methods have been done.[1–3] These studies indicate that the LBE produces accurate results comparable with traditional methods. As an approximate model of

[1] Center for Nonlinear Studies and Theoretical Division, Los Alamos National Laboratory, Los Alamos, New Mexico 87545.

[2] Department of Mathematics, Kansas State University, Manhattan, Kansas 66506.

[3] Department of Mechanical Engineering, Kansas State University, Manhattan, Kansas 66506.

[4] IBM Research Division, T. J. Watson Research Center, Yorktown Heights, New York 10598.

0022-4715/95/1000-0035$07.50/0

the Navier–Stokes equations, the LBE has two types of errors: errors due to the finite size of the lattice and errors due to compressibility effects. It is in the limit that lattice unit goes to zero (or lattice size goes to infinity) and Mach number (or velocity) does to zero that the LBE models the Navier–Stokes equations. For a given Mach number, when the lattice unit is not too small, the error of the LBE is $O(\delta^2)$ in the lattice unit δ.[3,4] As the lattice unit becomes smaller, the compressibility error becomes dominant and the error does not change much with refinement of the lattice.[3] To further reduce the error, one must first reduce the Mach number and reduce the lattice unit. On the other hand, if the Mach number (hence the velocity) is reduced, for a fixed lattice unit (limited by the computer size), one must decrease the viscosity to model a flow with given Reynolds number. But the decrease of viscosity is restricted by stability. Hence, it seems that the compressibility error is inevitable for the LBE. In this paper, a new LBE model is proposed to reduce the compressibility error significantly for steady flows. Numerical simulations using the new model show improved accuracy.

2. TWO-DIMENSIONAL SQUARE LATTICE BOLTZMANN MODEL

The proposed model can be derived from any existing lattice Boltzmann equation with a BGK collision operator. To illustrate the derivation, we use a 2D square LBGK (the d2p9 model in ref. 5). A square lattice with unit spacing is used in which each node has eight nearest neighbors connected by eight links. There are two types of moving particles. Particles of type 1 move along the axes with speed $\mathbf{e}_{1i} = (\cos[\pi(i-1)/2], \sin[\pi(i-1)/2])$, $i = 1, 2, 3, 4$, and particles of type 2 move along the diagonal directions with speed $\mathbf{e}_{2i} = \sqrt{2}(\cos[\pi(i-\frac{1}{2})/2], \sin[\pi(i-\frac{1}{2})/2])$, $i = 1, 2, 3, 4$. Rest particles with speed zero are also allowed at each node. The occupations of the three types of particles are represented by the single-particle distribution function, $f_{\sigma i}(\mathbf{x}, t)$, where the subscript σ indicates the type of particle (0: rest; 1: type 1; 2: type 2) and i indicates the velocity direction ($i = 1, 2, 3, 4$ for type 1 and type 2 particles). The particle distribution function satisfies the following lattice Boltzmann equation with BGK collision operator written in physical units:

$$f_{\sigma i}(\mathbf{x} + \delta \mathbf{e}_{\sigma i}, t + \delta) - f_{\sigma i}(\mathbf{x}, t) = -\frac{1}{\tau}[f_{\sigma i}(\mathbf{x}, t) - f_{\sigma i}^{(0)}(\mathbf{x}, t)] \qquad (1)$$

where $f_{\sigma i}^{(0)}(\mathbf{x}, t)$ is the equilibrium distribution at $\mathbf{x}$, t and τ is the single relaxation time which fixes the rate of approach to equilibrium. We use a

small parameter δ explicitly in the equation; it can be viewed as a time step (in physical units) in the simulation. Its value also represents the value of the length of a lattice link. The density per node, ρ, and the macroscopic velocity, $\mathbf{u}$, are defined in terms of the particle distribution function by

$$\sum_{\sigma}\sum_{i} f_{\sigma i} = \rho, \qquad \sum_{\sigma}\sum_{i} f_{\sigma i}\mathbf{e}_{\sigma i} = \rho\mathbf{u} \tag{2}$$

The equilibrium distribution can be chosen in the following form for particles of each type (the model d2p9[5]):

$$\begin{aligned} f_{01}^{(0)} &= \tfrac{4}{9}\rho[1 - \tfrac{3}{2}\mathbf{u}\cdot\mathbf{u}] \\ f_{1i}^{(0)} &= \tfrac{1}{9}\rho[1 + 3(\mathbf{e}_{1i}\cdot\mathbf{u}) + \tfrac{9}{2}(\mathbf{e}_{1i}\cdot\mathbf{u})^2 - \tfrac{3}{2}\mathbf{u}\cdot\mathbf{u}] \\ f_{2i}^{(0)} &= \tfrac{1}{36}\rho[1 + 3(\mathbf{e}_{2i}\cdot\mathbf{u}) + \tfrac{9}{2}(\mathbf{e}_{2i}\cdot\mathbf{u})^2 - \tfrac{3}{2}\mathbf{u}\cdot\mathbf{u}] \end{aligned} \tag{3}$$

with

$$\sum_{\sigma}\sum_{i} f_{\sigma i}^{(0)} = \rho, \qquad \sum_{\sigma}\sum_{i} f_{\sigma i}^{(0)}\mathbf{e}_{\sigma i} = \rho\mathbf{u} \tag{4}$$

In the limit that the lattice units and the Mach number approach zero, the density and velocity satisfy the Navier–Stokes equation. The form of error terms and the derivation can be found in refs. 2, 6, and 7. The macroscopic equations derived from the LBGK model d2q9 are as follows:

The continuity equation:

$$\partial_t \rho + \nabla\cdot(\rho\mathbf{u}) = 0 + O(\delta^2) \tag{5}$$

The momentum equation:

$$\begin{aligned} \partial_t(\rho u_\alpha) + \partial_\beta(\rho u_\alpha u_\beta) = &-\partial_\alpha(c_s^2\rho) + \frac{2\tau - 1}{6}\delta\partial_\beta[\rho(\partial_\alpha u_\beta + \partial_\beta u_\alpha)] \\ &+ O(\delta u^3) + O(\delta^2) \end{aligned} \tag{6}$$

where c_s is the speed of sound and $c_s^2 = 1/3$ for the model. For small Mach number and small lattice unit δ, the terms $O(\delta u^3) + O(\delta^2)$ can be neglected. Thus, thus, the continuity equation has the exact form of the usual NS equations [with an error term $O(\delta^2)$], and the momentum equation (6) is very similar to but not exactly the same as the momentum equation of NS equations. The viscosity is $[(2\tau - 1)/6]\delta$. If the characteristic velocity of the flow to be simulated is U and the characteristic length is L which includes N lattice units, then $\delta = L/N$ and the Reynolds number of the flow is $Re = UL/\nu = 6UN/(2\tau - 1)$. In the incompressible limit, $\rho \to$ const and the

incompressible NS equations can be recovered by taking $\rho = \rho_0$ (a constant) except in the term where $c_s^2 \rho$ represents the pressure.

In the case of steady flow (consider steadiness during the derivation), the macroscopic equations of the LBGK with error term become

$$\nabla \cdot (\rho \mathbf{u}) = 0 + O(\delta^2) \tag{7}$$

$$\partial_\beta (\rho u_\alpha u_\beta) = -\partial_\alpha (c_s^2 \rho) + \frac{2\tau - 1}{6} \delta \partial_\beta \partial_\beta (\rho u_\alpha) + O(\delta^2) \tag{8}$$

Notice that the term $O(\delta u^3)$ in Eq. (6) does not appear, because it comes from a temporal derivative. Comparing to the exact from of the steady incompressible NS equations at constant density ρ_0

$$\nabla \cdot \mathbf{u} = 0 \tag{9}$$

$$\partial_\beta (u_\alpha u_\beta) = -\partial_\alpha \left(\frac{p}{\rho_0} \right) + \nu \partial_{\beta\beta} u_\alpha \tag{10}$$

we see that terms containing the spatial derivative of ρ are neglected. For example, the continuity equation (7), $\nabla \cdot (\rho \mathbf{u}) = 0$ gives $\rho \nabla \cdot \mathbf{u} + (\nabla \rho) \cdot \mathbf{u} = 0$. When this is used to approximate Eq. (9), the term $(\nabla \rho) \cdot \mathbf{u}$ is neglected. This term represents a compressibility error. Since the order of magnitude of $\nabla \rho / \rho$ is $O(M^2)$,[1] where M is the Mach number, for a finite Mach number used in any simulation, a compressibility error appears. In a simulation of a 2D square cavity flow with a moving top by LBGK,[2] we consider this error by investigating the stream function $\psi(x, y)$: $\psi = \int_0^x -u_y \, dx$. For real, incompressible flow, the stream function should be zero at the walls; hence $\int_0^L u_y \, dx = 0$, where L is the length of a side of the square cavity. In our simulation, however, $\int_0^L u_y \, dx \neq 0$, because of the compressibility error. We calculate the stream functions $\psi(i, j)$ on the lattice with i, j representing different nodes. The mean and maximum stream functions at the right edge of the cavity are defined, respectively, as

$$S_\alpha = \left[\frac{\sum_{j=1}^{n_y} (\psi^2(n_x, j))}{n_y} \right]^{1/2} \qquad \text{and} \qquad S_m = \max_j |\psi(n_x, j)|$$

where $n_x = n_y = 256$ is the number of nodes in the x and y directions, respectively. An example of the error is presented in Table I, where U is the velocity of the top. The results show that S_α and S_m are proportional to M^2. We can use S_a and S_m as quantitative measures of the compressibility error of the LBE method. When the lattice unit decreases, the compressibility error may dominate.[3, 8]

Table I. Compressibility Error for d2q9, Re = 100

U	0.1	0.05	0.01
M	0.173	0.0867	0.0173
S_a	2.4×10^{-4}	6.4×10^{-5}	2.7×10^{-6}
S_m	6.7×10^{-4}	1.8×10^{-4}	8.1×10^{-6}

3. A NEW LBGK MODEL FOR STEADY INCOMPRESSIBLE FLOWS

In this section, a new LBGK model, which greatly reduces compressibility error for steady flows, is proposed. As Frisch *et al.*[9] pointed out, if one uses the mass current $\mathbf{v} = \rho \mathbf{u}$ to represent the velocity, then in the steady state the continuity equation implies exactly $\nabla \cdot \mathbf{v} = 0$. This formalism was used in lattice gas automata (see, for example, refs 10 and 11). If one uses $\mathbf{v}$ as the velocity, in the momentum equation, the viscous term is also exact, but the nonlinear term is not exactly equal to $\partial_\beta(v_\alpha v_\beta)$. In LGA, the nonlinear term can be approximated by $[g(\rho_0)/\rho_0]\,\partial_\beta(v_\alpha v_\beta)$ with a compressibility error from ignoring the change of ρ in this term. In the lattice Boltzmann method, however, the nonlinear term can be made exact by modifying the equilibrium distribution. The idea was used in ref. 12 to derive the exact form of the nonlinear term of the Burger's equation. We find that if the equilibrium distribution is chosen as

$$\begin{aligned} f_{01}^{(0)} &= \tfrac{4}{9}[\rho - \tfrac{3}{2}\mathbf{v}\cdot\mathbf{v}] \\ f_{1i}^{(0)} &= \tfrac{1}{9}[\rho + 3\mathbf{e}_{1i}\cdot\mathbf{v} + \tfrac{9}{2}(\mathbf{e}_{1i}\cdot\mathbf{v})^2 - \tfrac{3}{2}\mathbf{v}\cdot\mathbf{v}] \\ f_{2i}^{(0)} &= \tfrac{1}{36}[\rho + 3\mathbf{e}_{2i}\cdot\mathbf{v} + \tfrac{9}{2}(\mathbf{e}_{2i}\cdot\mathbf{v})^2 - \tfrac{3}{2}\mathbf{v}\cdot\mathbf{v}] \end{aligned} \tag{11}$$

with

$$\sum_\sigma \sum_i f_{\sigma i}^{(0)} = \rho, \qquad \sum_\sigma \sum_i f_{\sigma i}^{(0)} \mathbf{e}_{\sigma i} = \mathbf{v} \tag{12}$$

then using the LBGK equation (1) with

$$\sum_\sigma \sum_i f_{\sigma i} = \rho, \qquad \sum_\sigma \sum_i f_{\sigma i} \mathbf{e}_{\sigma i} = \mathbf{v} \tag{13}$$

and using the same procedure as before, we find the macroscopic equations of this new LBGK model for the steady case:

$$\nabla \cdot \mathbf{v} = 0 + O(\delta^2) \tag{14}$$

$$\partial_\beta(v_\alpha v_\beta) = -\partial_\alpha(c_s^2 \rho) + \frac{2\tau - 1}{6}\delta\partial_\beta\partial_\beta v_\alpha + O(\delta^2) \tag{15}$$

Apart from an error of $O(\delta^2)$ due to a finite lattice size, these are exactly the incompressible NS equations. The compressibility error induced by ignoring the change of density in the continuity equation and in some terms of the momentum equation no longer exists. Actually, it should be noted that the relevant fields for lattice Boltzmann methods are the momentum and pressure. The implementation of the new model (called d2q9i to be consistent with ref. 5) is almost the same as in the d2q9 model. For the 2D cavity flow, the boundary condition on the top is $v_x = U$ (U is the velocity of the moving top) and on other three walls, $\mathbf{v} = 0$ is obtained by using bounce-back conditions.

It is noted that the present model is only for steady flows. It cannot be extended to unsteady flows. The major problem is that the temporal derivative of ρ in the continuity equation is nonzero; it is related to the temporal derivative of pressure and it cannot be easily handled.

4. COMPUTATIONAL RESULTS

We give a comparison of the modified model (d2q9i) and the original model (d2q9) in the 2D square driven cavity flow and in a flow which has an analytic solution.

First, for d2q9i in 2D driven cavity flows, we use the following criterion to determine the steady state

$$\begin{aligned}&\left[\sum_i \sum_j |v_x(i, j, t+200) - v_x(i, j, t)|\right.\\ &\qquad \left. + |v_y(i, j, t+200) - v_y(i, j, t)|\right]\\ &\qquad \times \left[\sum_i \sum_j |v_x(i, j, t)| + |v_y(i, j, t)|\right]^{-1}\\ &\leqslant 10^{-6}\end{aligned}$$

where v_x, v_y are two components of the velocity $\mathbf{v}$. The maximum value of the stream function at the right wall (defined as S_m in Table I) is shown in Table II. The simulation is for $nx = ny = 256$, $U = 0.1$. We see the compressibility error in d2q9i is reduced drastically and the nonzero value of the stream function at the right wall is in the range of the numerical

Table II. Comparison of Compressibility Error S_m for Two Models

Model	Re = 100	Re = 1000
d2q9	6.7e−4	3.2e−4
d2q9i	6.8e−9	3.9e−9

integration error and the roundoff error.[2] We also compare other quantities. Table III is a comparison of the stream function at vortex centers (main, left, right) for the results by Ghia *et al.*,[13] d2q9, and d2q9i. The results are very close. In the new model, the error term related to ν does not appear explicitly, but the magnitude of ν is restricted by stability considerations. Nevertheless, the restriction is much less severe than that in d2q9. We did an experiment to increase U while fixing $\tau = 1$ to increase the Reynolds number. For the new model, the result of major quantities such as the value of the stream functions at vortex centers and the location of vortex centers are good up to $U = 0.5$. In contrast, $U = 0.5$ caues d2q9 to blow up. Hence, the new model is more robust.

To give a more detailed comparison, we consider a flow with an analytic solution. We choose a periodic flow so that the error on boundary condition is not present. The flow is in a square region $x \in [0, 2\pi]$, $y \in [0, 2\pi]$, with x and y velocities and pressure given by

$$u_x = u_0 \sin x \sin y, \quad u_y = u_0 \cos x \cos y, \quad p = \tfrac{1}{4}\rho_0 u_0^2(\cos 2x - \cos 2y) \tag{16}$$

where u_0, ρ_0 are constants. This is the exact solution of the steady incompressible NS equation with constant density ρ_0 and with a body force given by

$$F_x = 2\nu u_0 \sin x \sin y, \qquad F_y = 2\nu u_0 \cos x \cos y \tag{17}$$

Table III. Stream Function at Vortex Centers

Re	Model	ψ, main	ψ, left	ψ, right
100	Ghia	0.1034	−1.75e−6	−1.25e−5
	d2q9	0.1001	−1.76e−6	−1.14e−5
	d2q9i	0.1003	−1.79e−6	−1.15e−5
1000	Ghia	0.1179	−2.31e−4	−1.75e−3
	d2q9	0.1178	−2.22e−4	−1.69e−3
	d2q9i	0.1180	−2.24e−4	−1.70e−3

To incorporate a body force in LBGK, we add a term in the LBGK model, Eq. (1):

$$f_{\sigma i}(\mathbf{x}+\delta \mathbf{e}_{\sigma i}, t+\delta)-f_{\sigma i}(\mathbf{x}, t)=-\frac{1}{\tau}\left[f_{\sigma i}(\mathbf{x}, t)-f_{\sigma i}^{(0)}(\mathbf{x}, t)\right]+\delta g_{\sigma i}(\mathbf{x}, t) \quad (18)$$

For d2q9, $g_{\sigma i}$ is chosen as[6]

$$g_{01}=0, \qquad g_{1i}=\tfrac{1}{3}\rho e_{1i\alpha}F_\alpha, \qquad g_{2i}=\tfrac{1}{12}\rho e_{2i\alpha}F_\alpha \quad (19)$$

so that

$$\sum_\sigma\sum_i g_{\sigma i}=0, \qquad \sum_\sigma\sum_i g_{\sigma i}\mathbf{e}_{\sigma i}=\rho\mathbf{F}, \qquad \sum_\sigma\sum_i g_{\sigma i}e_{\sigma i\alpha}e_{\sigma i\beta}=0$$

where $\mathbf{F}$ is the body force. If we derive the macroscopic equation as before, an extra body force term ρF_α will appear in the momentum equation (6). For d2q9i, $g_{\sigma i}$ is chosen in a similar way but without ρ in the expression.

To start the simulation, we first compute the equilibrium distribution by using $\mathbf{u}$ of the exact solution and using $\rho=\rho_0+p/c_s^2$ for d2q9 and $\rho=\rho_0+p/(\rho_0 * c_s^2)$ for d2q9i with $c_s^2=1/3$ and p given in Eq. (16). Then we set $f_{\sigma i}=f_{\sigma i}^{(0)}$ as the initial distribution. To determine if the steady state is reached, we use the following criterion:

$$\begin{aligned}&\left[\sum_i\sum_j |u_x(i,j,t+1)-u_x(i,j,t)|\right.\\ &\qquad\left.+|u_y(i,j,t+1)-u_y(i,j,t)|\right]\\ &\qquad\times\left[\sum_i\sum_j |u_x(i,j,t)|+|u_y(i,j,t)|\right]^{-1}\\ &\leqslant \delta\cdot\text{tolerance}\end{aligned} \quad (20)$$

The tolerance is chosen as 10^{-12} in most runs. In some runs, the tolerance is chosen as 10^{-8}, but experience indicates that there is no difference in the error of velocity at the steady state.

For $\mathrm{Re}=100$, $u_0=0.1$, $\rho_0=2.7$, we use both d2q9 and d2q9i to run the simulation to steady state. Then we compute L1 and L2 relative errors err_1 and err_2 of the steady velocity:

$$err_1\equiv\frac{\sum_i\sum_j |u_x'(i,j)-u_x(i,j)|+|u_y'(i,j)-u_y(i,j)|}{\sum_i\sum_j |u_x'(i,j)|+|u_y'(i,j)|} \quad (21)$$

$$err_2\equiv\left\{\frac{\sum_i\sum_j [u_x'(i,j)-u_x(i,j)]^2+[u_y'(i,j)-u_y(i,j)]^2}{\sum_i\sum_j u_x'(i,j)^2+u_y'(i,j)^2}\right\}^{1/2} \quad (22)$$

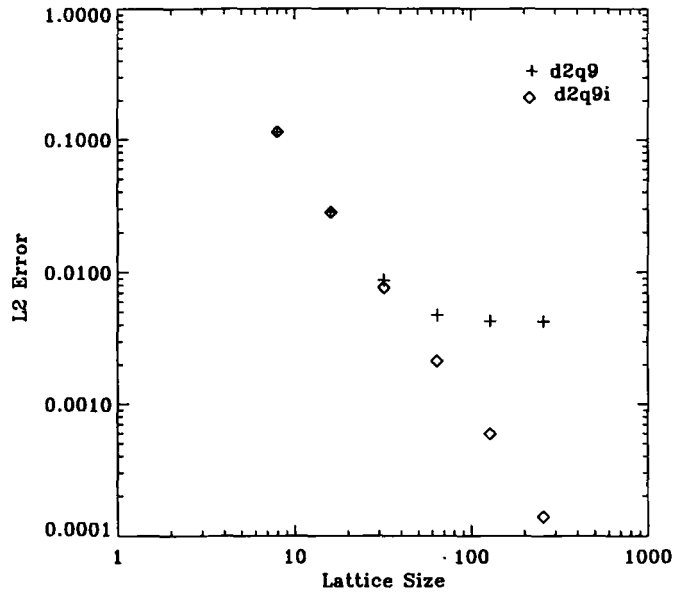

Fig. 1. L2 errors of velocity for two models.

where u_x^t and u_y^t are the analytical solution. The L1 and L2 relative errors of steady pressure are defined as

$$err_1 \equiv \frac{\sum_i \sum_j |p^t(i,j) - p(i,j)|}{\sum_i \sum_j |p^t(i,j)|} \tag{23}$$

$$err_2 \equiv \left\{ \frac{\sum_i \sum_j [p^t(i,j) - p(i,j)]^2}{\sum_i \sum_j p^t(i,j)^2} \right\}^{1/2} \tag{24}$$

where p^t is from the analytical solution given in Eq. (16). In d2q9, the pressure p is represented by $c_s^2(\rho - \rho_0)$, while in d2q9i, we used that $c_s^2(\rho - \rho_0) = p/\rho_0$.

The L2 relative error of velocity is shown in Fig. 1 (the behavior of the L1 error is similar). As the lattice size (number of lattice units on one side) increases from 8 to 256, the errors of d2q9 decrease initially as a second-order scheme.[3] Then the error levels off as lattice unit becomes smaller and the compressibility error becomes dominant. In contrast, the error of d2q9i continues to decrease as lattice unit decreases.

We also find that d2q9i is less sensitive to the magnitude of the velocity and has a slightly better stability behavior. We studied cases for which $\mathrm{Re} = 100$, $nx = ny = 128$; $\rho_0 = 2.7$; $u_0 = 0.1$, 0.2, 0.4, 0.5, 0.6, 0.7, and

0.8; tolerance $= 10^{-8}$. The initial distribution is the equilibrium distribution computed from the density and velocity of the analytical solution (we will refer to this later as initial distribution 1). The results for the L2 relative error of velocity and pressure in the steady state are shown in Tables IV and V, respectively. The L2 error of velocity and pressure in d2q9 increases as u_0 increases, indicating a compressibility error. The velocity error in d2q9i decreases slightly as u_0 increases from 0.1 to 0.4. Then it increases above $u_0 = 0.4$. The rate of increase of the error is much smaller than that of d2q9, and the model d2q9i has no instability up to $u_0 = 0.7$, indicating a slightly better stability behavior. The pressure error of d2q9i increases as u_0 increases; the increase is much slower than that in d2q9. Simulations for these parameters were performed also using for the initial distribution the equilibrium distribution computed from the density of the analytical solution and zero velocity (this is called initial distribution 2). This initial distribution is much different from the steady-state distribution. The time steps required to reach the steady state with a tolerance of 10^{-8} and for two different initial distributions are given in Table VI. It is seen that simulations with initial conditions closer to the steady-state solution reach the steady state faster. The case of $u_0 = 0.8$ for d2q9i is an interesting one. It reached the steady state for initial distribution 1 with a tolerance of 10^{-8}; but it did not reach the steady state for a tolerance of 10^{-12}. The minimum relative difference between the velocities at two consecutive time steps during the run was $9.25e-11$. However, if the initial distribution 2 was used, the system did not reach the steady state even for a tolerance of 10^{-8}. The minimum relative difference between the velocities at two consecutive time steps during the run was $1.26e-9$ (still larger than $\delta \cdot$ tolerance). For the case of $u_0 = 0.8$, when the solution did not reach the steady state, it wandered away and became unstable. For the case $u_0 = 0.7$ of d2q9i, if the tolerance was set to 10^{-12} then it did not reach the steady-state. The minimum relative difference between the velocities at two consecutive times steps is $7.55e-13$ for initial distribution 1 and $1.84e-11$ for initial distribution 2. Then the relative difference started to grow and eventually reached a nearly periodic state around $2.0e-2$. The method is still considered stable for this case. On the other hand, for the case $u_0 = 0.6$ of

Table IV. L2 Relative Error of Velocity as u_0 Increases, Re = 100[a]

u_0	0.1	0.2	0.4	0.5	0.6	0.7	0.8
d2q9	$0.428E-02$	$0.172E-01$	$0.744E-01$	0.128	NaN	NaN	NaN
d2q9i	$0.595E-03$	$0.557E-03$	$0.217E-03$	$0.949E-03$	$0.192E-02$	$0.312E-02$	NaN
d2q9w	$0.595E-03$	$0.557E-03$	$0.217E-03$	$0.949E-03$	$0.192E-02$	$0.312E-02$	NaN

[a] NaN (not a number) indicates overflow in the simulation.

Table V. L2 Relative Error of Pressure as u_0 Increases, Re = 100[a]

u_0	0.1	0.2	0.4	0.5	0.6	0.7	0.8
d2q9	0.391E−02	0.188E−01	0.920E−01	0.173	NaN	NaN	NaN
d2q9i	0.123E−02	0.265E−02	0.103E−01	0.159E−01	0.224E−01	0.295E−01	NaN
d2q9w	0.123E−02	0.265E−02	0.103E−01	0.159E−01	0.224E−01	0.295E−01	NaN

[a] NaN (not a number) indicates overflow in the simulation.

d2q9 with initial distribution 1, the minimum relative difference between the velocities at two consecutive time steps was only 3.20e−3 and the solution became unstable later. Hence, d2q9i has a slightly better stability than d2q9. We also studied the case of Re = 100, $nx = ny = 32$, $u_0 = 0.1$ ($\tau = 0.596$), tolerance of 10^{-20} with d2q9i. In this case, the steady state was never reached. The difference between the velocities at two consecutive time steps reached a minimum of 2.18e−14 and then it grew and eventually settled down around 4.0e−3 with a periodic behavior. The solution for the case with the same parameters except Re = 20 settled down to the steady state with the relative difference around 10^{-15}.

From these examples, it is seen that the solution can approach the steady-state solution and then diverge from it. How close the solution gets to the state-state solution depends on the parameters. An explanation for this behavior is that the steady state solution of Eq. (18) is a unstable fixed point of the dynamical system for a range of parameters. This unstable fixed point behaves like a saddle point. However, a full study of these effects is beyond the scope of this paper.

Table VI. Time Steps to Reach Steady State as u_0 Increases, Re = 100[a]

u_0	0.1	0.2	0.4	0.5	0.6	0.7	0.8
d2q9(I.D. 1)	8902	5493	4212	NaN	NaN	NaN	
d2q9(I.D. 2)	22907	12246	6937	5931	NaN	NaN	NaN
d2q9i(I.D. 2)	8825	4806	3315	3013	2630	2188	2715
d2q9i(I.D. 2)	22908	12242	6886	5881	5275	4891	NaN

[a] I.D. 1, 2 represent initial distributions 1 and 2, respectively.

Some studies were carried out to study the effect of changes in density. For this purpose, we tried another model, which is also based on the LBGK equation, Eq. (18), with the following equilibrium distribution:

$$\begin{aligned} f_{01}^{(0)} &= \tfrac{4}{9}[\rho - \tfrac{3}{2}\rho_0 \mathbf{w}\cdot\mathbf{w}] \\ f_{1i}^{(0)} &= \tfrac{1}{9}[\rho + 3\rho_0 \mathbf{e}_{1i}\cdot\mathbf{w} + \tfrac{9}{2}\rho_0(\mathbf{e}_{1i}\cdot\mathbf{w})^2 - \tfrac{3}{2}\rho_0\mathbf{w}\cdot\mathbf{w}] \\ f_{2i}^{(0)} &= \tfrac{1}{36}[\rho + 3\rho_0 \mathbf{e}_{2i}\cdot\mathbf{w} + \tfrac{9}{2}\rho_0(\mathbf{e}_{2i}\cdot\mathbf{w})^2 - \tfrac{3}{2}\rho_0\mathbf{w}\cdot\mathbf{w}] \end{aligned} \tag{25}$$

The structure of $f_{\sigma i}^{(0)}$ is similar to that of d2q9 with

$$\sum_\sigma \sum_i f_{\sigma i} = \sum_\sigma \sum_i f_{\sigma i}^{(0)} = \rho, \qquad \sum_\sigma \sum_i f_{\sigma i}\mathbf{e}_{\sigma i} = \sum_\sigma \sum_i f_{\sigma i}^{(0)}\mathbf{e}_{\sigma i} = \rho_0 \mathbf{w} \tag{26}$$

and $g_{\sigma i}$ is given in Eq. (19) with ρ being replaced by ρ_0. The velocity is represented by $\mathbf{w}$, and the macroscopic equation in the steady case for his model is

$$\nabla\cdot\mathbf{w} = 0 + O(\delta^2) \tag{27}$$

$$\partial_\beta(w_\alpha w_\beta) = -\partial_\alpha\left(c_s^2\frac{\rho}{\rho_0}\right) + \frac{2\tau-1}{6}\delta\partial_\beta\partial_\beta w_\alpha + O(\delta^2) \tag{28}$$

The results for the model d2q9w are listed in Tables IV and V for the same parameters. The relative errors of velocity and pressure in d2q9w are identical to those in d2q9i. We note that in the incompressible NS equation with constant density, ρ_0 is not a relevant variable and can be absorbed into pressure to form an effective pressure $\bar{p} \equiv p/\rho_0$. In d2q9 and d2q9w, we use $c_s^2(\rho - \rho_0)/\rho_0 = \bar{p}$ while in d2q9i, we use $c_s^2(\rho - \rho_0) = \bar{p}$. With this in mind, we observed the following:

1. In models d2q9 and d2q9w, a scaling of ρ_0 amounts to scaling $f_{\sigma i}^{(0)}$, $f_{\sigma i}$ and ρ for fixed velocity and effective pressure $\bar{p}$. The scaled $f_{\sigma i}^{(0)}$ and $f_{\sigma i}$ still satisfy the LBGK equation (18). Any change in ρ_0 does not change the velocity or effective pressure. Hence, ρ_0 is an irrelevant parameter for both the d2q9 and d2q9w models.

2. For models d2q9i with $f_{\sigma i}, f_{\sigma i}^{(0)}$ corresponding to ρ_0, ρ, and velocity $\mathbf{v}$, if ρ_0 is changed to $\rho_0 + \Delta\rho$, where $\Delta\rho$ is a constant, and new distribution functions $\bar{f}_{\sigma i}$, $\bar{f}_{\sigma i}^{(0)}$ are defined as

$$\bar{f}_{\sigma i} = f_{\sigma i} + t_\sigma \Delta\rho; \quad \bar{f}_{\sigma i}^{(0)} = f_{\sigma i}^{(0)} + t_\sigma \Delta\rho; \quad t_0 = \tfrac{4}{9}, \quad t_1 = \tfrac{1}{9}, \quad t_2 = \tfrac{1}{36} \tag{29}$$

then $\bar{f}_{\sigma i}$ and $\bar{f}_{\sigma i}^{(0)}$ still satisfy the LBGK equation (18), giving the same velocity and effective pressure. That is, the change of ρ_0 does not affect the

velocity and effective pressure. Hence, ρ_0 is also an irrelevant parameter for the d2q9i model.

3. The models d2q9i and d2q9w with the same u_0, τ and ρ_0 are identical if the following normalized distribution $\bar{f}_{\sigma i}$ is used: for d2q9i, $\bar{f}_{\sigma i}$ is given by Eq. (29) with $\Delta\rho = -\rho_0$; for d2q9w, $\bar{f}_{\sigma i} = f_{\sigma i}/\rho_0 - t_\sigma$ with t_σ given in Eq. (29).

The linear stability analysis by Sterling *et al.*[7] indicates that the stability of d2q9 depends on τ, u_0, the ratio between distributions of rest particles and moving particles, and the wavenumber. The stability of d2q9 is independent of the density.

5. CONCLUSION

We have presented an improed LBGK model for steady incompressible flows. This model reduces the compressibility error significantly and is more robust.

ACKNOWLEDGMENTS

We would like to thank Y. H. Qian, H. Chen, J. Sterling, M. Reider, L. S. Luo, X. Shan, S. Succi, J.-P. Rivet, B. Nadiga, and P. Skordos for helpful discussions. We also would like to thank an anonymous referee for many helpful comments and suggestions. Q. Z. would like to thank the Associated Western Universities Inc. for providing a fellowship to him.

REFERENCES

1. D. O. Martinez, W. H. Matthaeus, S. Chen, and D. C. Montgomery, *Phys. Fluids* **6**(3):1285 (1994).
2. S. Hou, Q. Zou, S. Chen, G. D. Doolen, and A. C. Cogley, *J. Comput. Phys.* **118**:329 (1995).
3. M. B. Reider and J. D. Sterling, Accuracy of discrete-velocity BGK models for the simulation of the incompressible Navier–Stokes equations, *Computers Fluids*, to appear (1995).
4. B. H. Elton, Comparisons of lattice Boltzmann methods and a finite-difference method for a two-dimensional viscous Burgers equation, submitted.
5. Y. Qian, D. d'Humières, and P. Lallemand, *Europhys. Lett.* **17**(6):479 (1992).
6. Y. Qian, Ph.D. thesis, Université Pierre et Marie Curie (January 1990).
7. J. D. Sterling and S. Chen, Stability analysis of the lattice Boltzmann method, *J. Comput. Phys.*, to appear (1995).
8. P. A. Skordos, *Phys. Rev. E* **48**:6 (1993).
9. U. Frisch, D. d'Humières, B. Hasslacher, P. Lallemand, Y. Pomeau, and J.-P. Rivet, *Complex Systems* **1**:649 (1987).

10. D. d'Humières and P. Lallemand, *Complex Systems* 1:599 (1987).
11. L. P. Kadanoff, G. R. McNamara, and G. Zanetti, *Complex Systems* **1**:791 (1987).
12. F. J. Alexander, H. Chen, S. Chen, and G. D. Doolen, *Phys. Rev. A* **46**:1967 (1992).
13. U. Ghia, K. N. Ghia, and C. Y. Shin, *J. Comput. Phys.* **48**:387 (1982).
14. Y. H. Qian and S. A. Orszag, *Europhys. Lett.* **21**(3):255 (1993).